

Multimodal Real-Time patient emotion recognition system using facial expressions and brain EEG signals based on Machine learning and Log-Sync methods

A.M. Mutawa^{*}, Aya Hassouneh

Dept. of Computer Engineering, College of Engineering and Petroleum, Kuwait University, Kuwait

ARTICLE INFO

Keywords:

EEG
Multi-modal
Neural network
Log-sync
Face recognition
Emotion recognition
Hospitalized patients

ABSTRACT

Human Machine Interface (HMI) depends on emotion detection, especially for hospitalized patients. The emergence of the fourth industrial revolution (4IR) has heightened the interest in emotional intelligence in human–computer interaction (HCI). This work employs electroencephalography (EEG), an optical flow algorithm, and machine learning to create a multimodal intelligent real-time emotion recognition system. The objective is to assist hospitalized patients, disabled (deaf, mute, and bedridden) individuals, and autistic youngsters in expressing their authentic feelings. We fed our multimodal feature fusion vector to a classifier with long short-term memory (LSTM). We distinguished six fundamental emotions: anger, disgust, fear, sadness, joy, and surprise. The fusion feature vector was created utilizing the patient's geometric facial characteristics and EEG inputs. Utilizing 14 EEG inputs, we used four-band relative power channels, namely alpha (8–13 Hz), beta (13–30 Hz), gamma (30–49 Hz), and theta (4–8 Hz). We achieved a maximum recognition rate of 90.25 percent using just facial landmarks and 87.25 percent using only EEG data. When both facial and EEG streams were examined, we achieved 99.3 percent accuracy in a multimodal method.

1. Introduction

Facial expression recognition is one of the most efficient, significant, natural, and rapid ways in which people communicate emotions and intentions. Due to deficiencies or illnesses, some individuals cannot communicate their emotions in specific situations, such as when they are in pain, discouraged, or uncomfortable [1]. The more successfully we can transform the patient's emotional experience into useful information, the more we can assist the patient in these situations. Therefore, it is vital to comprehend emotional expressions in order to communicate properly.

Human emotions are a critical communication tool [2]. If understood, they may be utilized to influence and increase productivity in a variety of applications [3]. Because the strength of emotions vary from person to person, emotion identification necessitates the integration of several data sources [4]. Thus, many studies employ voice messages, facial expressions, gestures, statistics, and other kinds of emotional data to determine emotions [5–12].

Some research utilize voice to identify emotions [13–15], while others mix speech and text [7,16] or both inputs with facial

characteristics [17,18]. Even though a few studies use video clips to measure emotions [19–22], it has been shown that using several modes improves recognition. [5,23,24].

Recent research has focused on the capacity of EEG head signals to comprehend and capture human emotions [20,25–29]. One example of this is the application of the theory of perceptual control, which discusses how the brain regulates human behavior and perception by controlling sensory input [30]. This can be achieved using wearable sensor-based devices, which provide continuous and non-intrusive monitoring of bodily functions [31]. In addition to this, CT images have been used to predict the severity of COVID-19 with high accuracy [32]. The model achieved a 99.0 percent accuracy in predicting the severity of COVID-19. Furthermore, a new chaotic optimization algorithm based on biogeography-based optimization has been proposed [33]. This algorithm has potential applications in various fields, including EEG signal analysis, for feature selection purposes.

The most current EEG-based strategies are outlined in Table 1. Several studies have exploited the holographic and topographic features of EEG signals with an accuracy of 88 percent [28] while others have trained EEG data from the left and right hemispheres separately to verify

^{*} Corresponding author.

E-mail addresses: dr.mutawa@ku.edu.kw (A.M. Mutawa), aia.hassouneh@gmail.com (A. Hassouneh).

Table 1
EEG-based related work to detect emotions using different approaches.

Reference	Features Used	ML Model Used	Max Accuracy
[6]	EEG signals	LSTM and GCNN fusion	90.06 %
[7]	EEG & textual-based feature	CNN and SVM	81 %
[28]	Multifeatured fusion holographic and topographic	CNN and SVM	88 %
[34,35]	EEG signals	BiDCNN	94.72 %
[35]	EEG and facial	CNN and Monte Carlo	88.33 %
[36,37]	EEG and facial features	LIBSVM and DNN	85.71 %
[3730323133]	EEG and facial features	Hierarchical models	95.08 %
	EEG signals	LEDPatNet19	99.29 %
	EEG signals	PrimePatNet87	99 %
	EEG signals	RFE + SVM	99.82 %
	EEG signals	SVM	

emotions using a discrepancy convolution neural network [34]. Reported identification rates of 83.33 percent [35], 85.71 percent [36], and 95.08 percent [37] were achieved when EEG and facial characteristics were used in conjunction with multimodal techniques to detect human emotion. Our research integrated EEG data and facial features but trained them using our novel log-sync method, yielding a 99.3 percent recognition rate.

The accuracy of recognition still has to be improved, even though numerous research have used a variety of data sources, such as voice

messages, facial expressions, gestures, and EEG signals. It is also vital to investigate ways to more effectively and efficiently integrate different data sources to improve the ability to recognize emotions. The log-sync mechanism employed in this study is one potential method for accomplishing this. The remaining sections are organized as follows: Methods are discussed next in section 2, followed by data collection in section 3. Section 4 displays the results and discussion, followed by the conclusions in section 5.

2. Materials and methods

2.1. Proposed multimodal structure

The suggested system structure is shown in Fig. 1. We applied two methods to determine the patients' emotions: (1) facial landmarks and (2) EEG signals. Each method generated a feature vector. We then combined both feature vectors to create a fusion vector. Finally, the LSTM classifier was applied to the fusion vector to identify the patient's emotions.

The Emotiv Epoc Device captures raw EEG data from 14 channels at a sampling rate of 128 Hz [38]. A spotter is positioned in front of the patient to record any changes in behavior throughout the duration of the films while watching them and clicking on the input device and synchronizing the time of the difference with the EEG signals obtained at the same event, as seen in Fig. 2. This spotter-log-synchronization approach is abbreviated as log-sync. All the symbols and other abbreviations used in this paper are listed in Table 2. The log-sync will add a new depth to the system during the training process, identifying when a

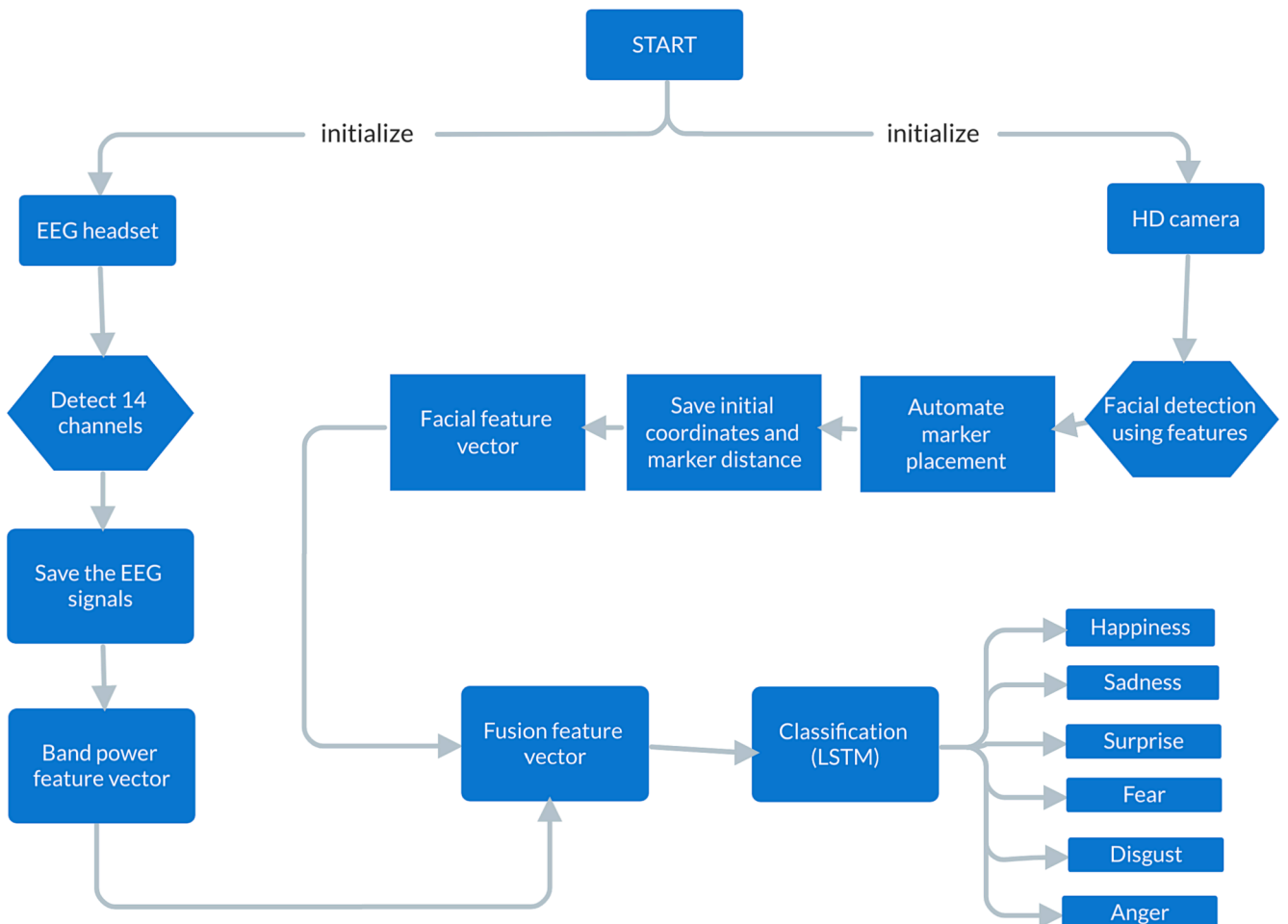


Fig. 1. System structure.

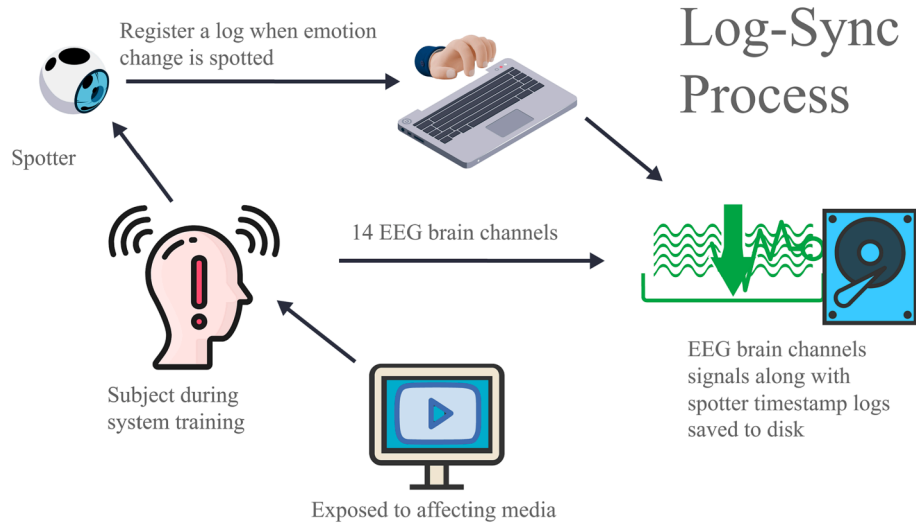


Fig. 2. Synchronizing the subject's reaction with the EEG signals during the data collection phase using the log-sync method.

Table 2

List of abbreviations and symbols we used in this paper.

Abbreviations and Symbols	Meaning
HMI	Human Machine Interface
4IR	Fourth Industrial Revolution
ML	Machine Learning
HCI	Human-Computer Interaction
EEG	Electroencephalogram
LSTM	Long Short-Term Memory
m_i	Marker Position
c_i	Center Position
FAFV	Facial Feature Vector
ts	Time Stamp
rd	Relevant Distance
BPFV	Band Power Feature Vector
FFT	Fast Fourier Transform
PSD	Power Spectral Density
rbp	Relative Band Power
FUFV	Fusion Feature Vector
RNN	Recurrent Neural Network
Log-sync	Spotter-Log-Synchronization Approach

person feigns emotion, which is when the EEG signals do not correspond to the appearance of the face. Typically, a skilled person could observe this intelligent behavior for close relatives and friends such as spouses or family members. Nonetheless, it might be difficult for others.

As for facial detection, there has been much work in the literature to automatically place markers on the face ranging from 10 to 68 markers [20,39–41]. We have implemented the work of Hassouneh [20] by placing 10 markers with a center marker at the nose, as shown in Fig. 3. Features are taken by calculating the absolute distance from each marker to the central point, as explained in the feature extraction section below.

2.2. Feature extraction

The fusion feature vector is constructed by combining the facial feature vector and the band power feature vector as depicted in Fig. 1 above.

2.2.1. Facial feature vector (FAFV)

For each of the ten virtual marker positions (m_1, m_2, \dots, m_{10}) shown in Fig. 3, a facial feature vector FAFV is composed of the time stamp, ts , in seconds followed by the relative distance, rd , from the center point C_{xy} , according to Equation (1) and Equation (2) below:

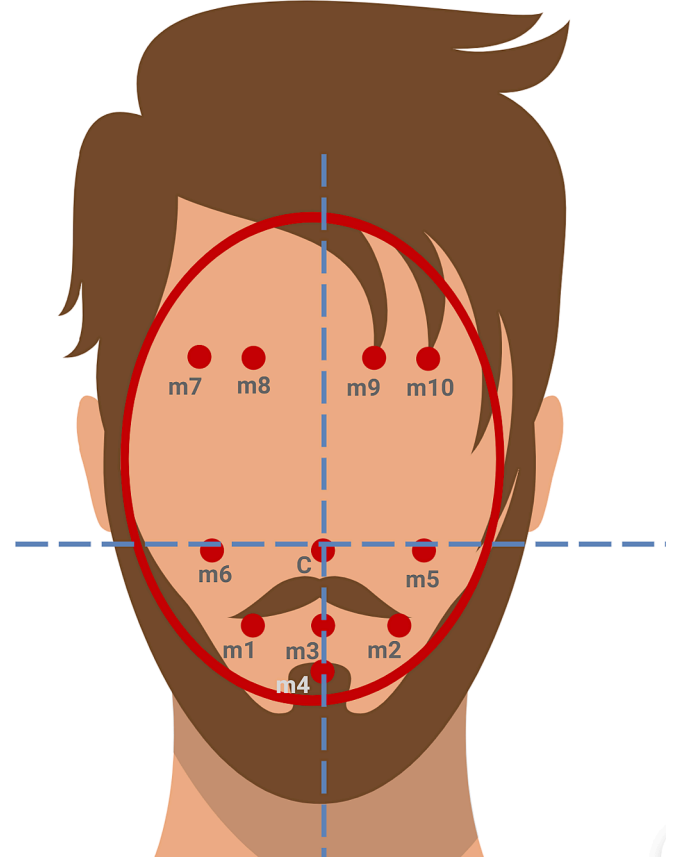


Fig. 3. Ten marker points m_1 to m_{10} and a center point C within an ellipse mapped on a human face.

$$rd_i = \sqrt{(C_x - m_{i,x})^2 + (C_y - m_{i,y})^2} \quad (1)$$

$$FAFV_i = (ts, rd_1, rd_2, \dots, rd_{10}) \quad (2)$$

2.2.2. Band power feature vector (BPFV)

The EEG signals are recorded using the Epoc + interface and transmitted wirelessly to the Emotiv Epoc application to be stored and saved on the drive for processing and feature extraction. The decomposition of

the signal into functionally separate frequency bands such as theta (4–8 Hz), alpha (8–12 Hz), beta (12–30 Hz), and gamma (30–50 Hz), is a frequently used approach for analyzing EEG data.

This entails decomposing the EEG signal into frequency components using the Fast Fourier Transform (FFT) algorithm, which produces a complex integer for each frequency bin. The amplitude and phase of the signal at that particular frequency may be readily extracted. The magnitude-squared of the FFT is then used to calculate the power spectral density, which is given in (micro)-Volts² per Hertz. Then the power spectral density (PSD) is based on the generalized formula for discrete-time series $x(t)$ shown in Equation (3), where N is big enough to include an entire wave cycle.

$$PSD_{f,x(t)} = \lim_{N \rightarrow \infty} \frac{\Delta f^2}{T} \left| \sum_{n=-N}^N x_n e^{-2\pi i n \Delta t} \right|^2 \quad (3)$$

Then we finally calculate the relative band power rbp by dividing the PSD by the sum of all bins within the range of our scope 4 Hz to 50 Hz to generate the band power feature vector (BPFV) along with the time stamp ts as in Equation (4).

$$BPFV_i = (ts, rbp_1, rbp_2, rbp_3, \dots, rbp_n) \quad (4)$$

2.2.3. Fusion feature vector (FUFV)

The fusion feature vector (FUFV) has offline and online operation modes. When the operation is offline, the generated data is stored on the drive for later processing to be used for machine learning to train the neural network, as explained in the classification section. When the operation is set to online mode, the generated vector FUFV is directly fed to the classifier without being stored on the drive.

During the training process, vectors FAFV and BPFV are synchronized with the log-sync signal to generate the extended FUFV as in Equation (5) with the log-sync tagged emotion based on the video segment displayed, as shown in Fig. 4.

$$FUFV_i = (ts, rd_1, \dots, rd_{10}, rbp_1, rbp_2, \dots, rbp_n, \log - sync_{tag}) \quad (5)$$

When operating in online mode, both streams are combined and aligned based on the time key value into one vector and then fed to the classifier without the log-sync tag as shown in Equation (6). The emotion E_i at an instant i is then recognized after applying the LSTM classifier on the multimodal vector MME_i , as shown in Equation (7).

$$MME_i = \begin{cases} \bigcup (FAFV_i, BPFV_i, LogSync_i) \forall i \in \text{offline} \\ \bigcup (FAFV_i, BPFV_i) \forall i \in \text{online} \end{cases} \quad (6)$$

$$E_i = LSTM(MME_i) \quad (7)$$

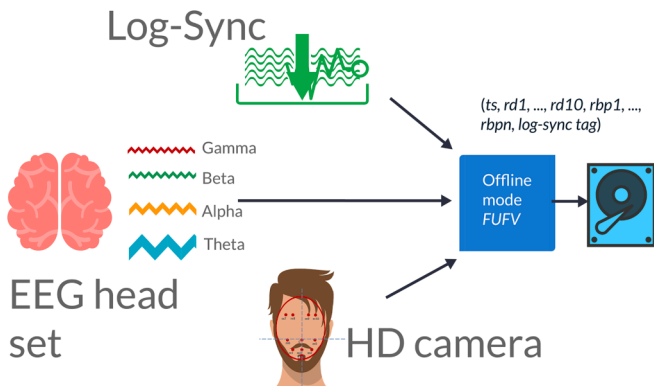


Fig. 4. Offline-mode fusion feature vector process.

2.3. Classification and validation

2.3.1. Data classification

We train our recurrent neural network (RNN) using long short-term memory (LSTM) classification to predict the patient's mood based on the input fusion vector. The fusion vector is fed into the embedding layer, followed by a 128-neuron LSTM layer, a 20 percent dropout layer, a second LSTM layer with half the number of neurons in the first layer, a second 20 percent dropout layer, and a third LSTM layer with half the number of neurons in the previous LSTM layer, followed by a second 20 percent dropout layer and a third LSTM layer with half the number of neurons in the last LSTM layer. The dropout layer helps in protecting our model against overfitting, where a certain percentage of neurons are randomly dropped out during training to prevent the model from becoming too reliant on any one feature.

For comparison purposes, we applied the training on FAFV and BPFV separately before implementing training on the multimodal vector FUFV.

2.3.2. Data validation

System validation aims to evaluate the accuracy after development. It was tested by finding data, especially for the testing.

The facial landmarks data for the 19 subjects are fed into the three-fold cross-validation method to split the features into training and testing sets. Thus, the proposed method achieves a higher emotion detection rate of 99.3 percent. Understanding that by splitting the dataset into training and validation sets, cross-validation can prevent our model from overfitting by allowing us to assess the model's performance on new data.

3. Data collection

Nineteen healthy volunteer subjects (7 males and 12 females) from a mean age domain of 22.9 years participated in this study after signing a consent form understanding their complete freedom and right to stop and depart at any time during the session if they feel uncomfortable or for any other reason with no obligation whatsoever. None of the participants were given any kind of honorarium or compensation for their time or efforts.

The most challenging component was exposing a subject to six distinct emotions in the same session through effective media that has been shown to affect the general public. As a result, we used two media sources for each emotion, one from YouTube and the other from the International Affective Picture System [42] combined with sound effects [43]. As for YouTube videos, a clip must accumulate at least one million views and has the reviewers' remarks accurately representing the emotion elicited by the research. A control group is exposed to the chosen media, followed by a brief survey to confirm, and verify the feeling. Once the average response exceeds the specified threshold, the video is retained in our list. This procedure is repeated until our inventory is complete for all six emotions.

The next stage is gathering facial and electroencephalographic (EEG) data from the participants exposed to our pre-selected videos. Each two-minute video clip focuses on a different feeling. The patient is repeatedly exposed to several videos within the same category, followed by a ten-second break before moving onto another two-minute clip in a new category. We took a 10-second break merely to figure out where to place the markers on the EEG signal and thus, identify the start and end of each emotion and be able to ignore the start and end in the event that the subject displayed the incorrect emotion or expression. All the individuals were instructed to view six 2-minute different videos to express the six emotions. Thus, each person needed 13 min to convey the six feelings.

The individuals' faces were captured and converted to grayscale using an HD camera. Then, a grayscale picture was utilized to identify the subject's eyes, and 10 virtual markers (action units) were placed at

specific positions on the subject's face, as shown in Fig. 3. Each virtual marker location was recorded on the hard drive using the Lucas-Kande optical flow algorithm to monitor its position throughout the emotional expression of the subject and then processed further. The combined data set consisted of all 14 EEG channel signals and the recorded facial landmarks for each of the 19 people, totaling 1,700,000 signal data recordings.

4. Experimental results and discussion

The accuracy of the facial landmarks gathered concurrently with the EEG signals of the 19 individuals was 87 percent. After normalization, it increased to 90 percent, whereas the accuracy of the EEG raw data was 83 percent. The data were then standardized, and the loss function was modified to achieve an accuracy of 87 percent. Additionally, the EEG accuracy improved proportionately when the number of epochs grew, as seen in Fig. 5, which illustrates the direct link between model accuracy and epoch count. These results are impressive, considering the complexity of the task and the challenges in collecting and processing multiple modalities.

However, the accuracy of the multimodal vectors, a concatenation of the four-band power derived from the EEG signals, and the ten virtual distances collected simultaneously from the subject's face while viewing the movie, is 99.3 percent. Fig. 6 illustrates the direct link between the number of epochs and the multimodal system's accuracy.

The study's limitations included the complexity of the system, the difficulty and time-consuming nature of collecting and labeling data for multiple modalities, and the limited generalizability of the system to different populations or settings due to variations in the features used to detect emotions. However, our system excels because it uses multiple modalities to capture complementary information about the emotions being expressed. The facial landmarks provide information about facial expressions, while the EEG signals provide information about the brain activity associated with emotions. By combining these modalities, we were able to capture a more comprehensive representation of emotions, resulting in a highly accurate emotion detection system.

Another advantage of our system is its robustness to variations in the data. Since we used multiple modalities, the system could rely on different sources of information to detect emotions. This robustness makes our system more adaptable and flexible, as it can be customized for different populations or settings by selecting the modalities that are most relevant to the specific task.

In conclusion, our study showed that the accuracy of emotion detection systems is greatly increased using several modalities. Our

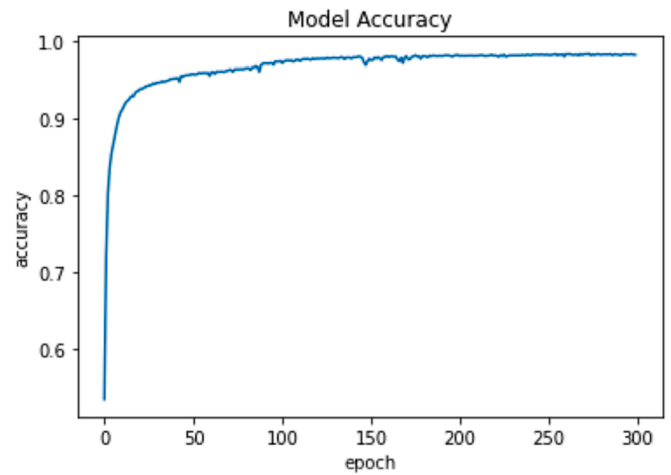


Fig. 6. Accuracy against epoch count for multi-model emotion detection system.

system's accuracy was determined to be very high. However, more research is required to examine its generalizability to various populations and environments.

5. Conclusion

A novel multimodal approach for in-patient emotion identification has been created. It uses facial and EEG brain signals to accurately portray patients' true feelings when they cannot express them due to medical issues or fake them to avoid essential treatments. Our approach was trained by confirming responses with a third human spotter using our log-sync tagging algorithm. Simultaneously, the individuals were exposed to a variety of video clips. Video clips were meticulously chosen from an international standard collection and famous video clips. A three-fold cross-validation approach was used to verify the training system.

The findings indicate that the system can recognize emotion in 99.3 percent of the cases when combined with facial landmarks and EEG inputs. The accuracy of face recognition alone was 90 percent, while the accuracy of EEG signals alone was 87 percent. Thus, a multimodal system outperformed a singleton system in terms of accuracy. Synthetically creating new samples from the existing ones can increase the size of the data set, which can help prevent overfitting.

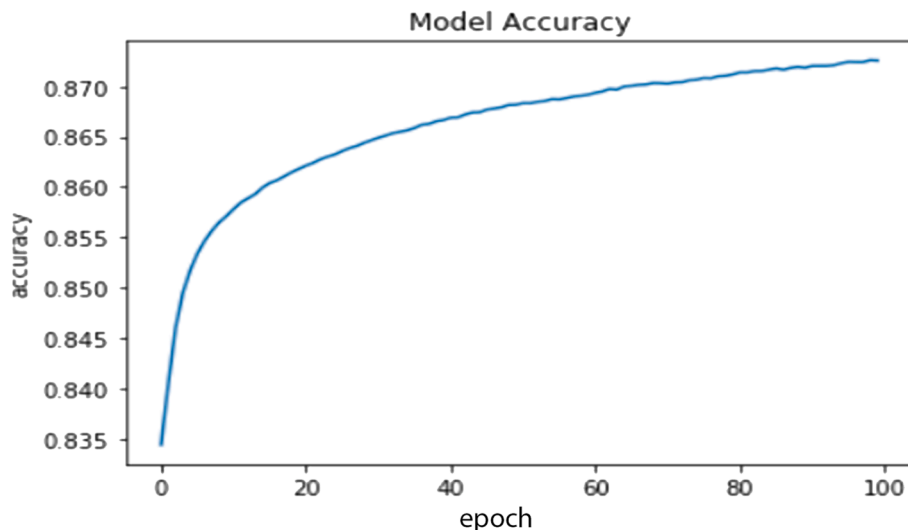


Fig. 5. Model accuracy against epoch count with EEG signal only.

For future studies, the precision and accuracy of the system may be increased by gathering data from a larger number of participants. Additionally, the system can be applied to a variety of other interesting, intelligent applications, such as self-learning distance education, where a student can be automatically directed to a fork of sequence learning materials based on their emotions, as indicated by their level of acceptance for whether the materials viewed were easily consumed or not.

CRedit authorship contribution statement

A.M. Mutawa: Conceptualization, Methodology, Formal analysis, Resources, Writing – review & editing, Visualization, Supervision, Project administration. **Aya Hassouneh:** Software, Validation, Investigation, Resources, Data curation, Writing – original draft.

Declaration of competing interest

The authors declare that they have no known competing financial interests or personal relationships that could have appeared to influence the work reported in this paper.

Data availability

Data will be made available on request.

Acknowledgements

Both authors would like to express their acknowledgment of the continuous support of the Kuwait University.

References

- [1] S. Hwang, J. Hwang, H. Jeong, Study on associating emotions in verbal reactions to facial expressions in Dementia, in *Healthcare* 10 (6) (2022) 1022. MDPI.
- [2] M. Liu et al., "Facial expressions elicit multiplexed perceptions of emotion categories and dimensions," *Current Biology*, vol. 32, no. 1, pp. 200–209. e6, 2022.
- [3] T. Gupta, C.M. Haase, G.P. Strauss, A.S. Cohen, J.R. Ricard, V.A. Mittal, Alterations in facial expressions of emotion: Determining the promise of ultrathin slicing approaches and comparing human and automated coding methods in psychosis risk, *Emotion* 22 (4) (2022) 714.
- [4] M.L. Dyer, A.S. Attwood, I.S. Penton-Voak, M.R. Munafo, The role of state and trait anxiety in the processing of facial expressions of emotion, *R. Soc. Open Sci.* 9 (1) (2022) 210056.
- [5] S.M.S.A. Abdullah, S.Y.A. Ameen, M.A. Sadeeq, S. Zeebaree, Multimodal emotion recognition using deep learning, *J. Appl. Sci. Technol. Trends* 2 (02) (2021) 52–58.
- [6] Y. Yin, X. Zheng, B. Hu, Y. Zhang, X. Cui, EEG emotion recognition using fusion model of graph convolutional neural networks and LSTM, *Appl. Soft Comput.* 100 (2021) 106954.
- [7] Y. Liu, G. Fu, Emotion recognition by deeply learned multi-channel textual and EEG features, *Futur. Gener. Comput. Syst.* 119 (2021) 1–6.
- [8] F.J. Otamendi, Statistical emotion control: Comparing intensity and duration of emotional reactions based on facial expressions, *Expert Syst. Appl.* 200 (2022) 117074.
- [9] M. Porta-Lorenzo, M. Vázquez-Enríquez, A. Pérez-Pérez, J.L. Alba-Castro, L. Docío-Fernández, Facial Motion Analysis beyond Emotional Expressions, *Sensors* 22 (10) (2022) 3839.
- [10] W. Ali, W. Tian, S.U. Din, D. Iradukunda, A.A. Khan, Classical and modern face recognition approaches: a complete review, *Multimed. Tools Appl.* 80 (3) (2021) 4825–4880.
- [11] L.R. Christensen, M.A. Abdullah, EEG emotion detection review, in: In 2018 IEEE Conference on Computational Intelligence in Bioinformatics and Computational Biology (CIBCB), 2018, pp. 1–7.
- [12] D. Li, B. Chai, Z. Wang, H. Yang, W. Du, EEG emotion recognition based on 3-D feature representation and dilated fully convolutional networks, *IEEE Trans. Cogn. Developm. Syst.* 13 (4) (2021) 885–897.
- [13] C. Guanghui, Z. Xiaoping, Multi-modal emotion recognition by fusing correlation features of speech-visual, *IEEE Signal Process Lett.* 28 (2021) 533–537.
- [14] P. Koromilas, T. Giannakopoulos, Deep multimodal emotion recognition on human speech: A review, *Appl. Sci.* 11 (17) (2021) 7962.
- [15] D.M. Schuller, B.W. Schuller, A review on five recent and near-future developments in computational processing of emotion in the human voice, *Emot. Rev.* 13 (1) (2021) 44–50.
- [16] W.Y. Choi, K.Y. Song, C.W. Lee, Convolutional attention networks for multimodal emotion recognition from speech and text data, in: In Proceedings of Grand Challenge and Workshop on Human Multimodal Language (challenge-HML), 2018, pp. 28–34.
- [17] T. Mittal, U. Bhattacharya, R. Chandra, A. Bera, D. Manocha, M3er: Multiplicative multimodal emotion recognition using facial, textual, and speech cues, *Proceedings of the AAAI Conference on Artificial Intelligence* 34 (02) (2020) 1359–1367.
- [18] J. Chen, T. Ro, Z. Zhu, Emotion recognition with audio, video, EEG, and EMG: A dataset and baseline approaches, *IEEE Access* 10 (2022) 13229–13242.
- [19] B. Pan, K. Hirota, Z. Jia, L. Zhao, X. Jin, Y. Dai, "Multimodal emotion recognition based on feature selection and extreme learning machine in video clips," *J. Amb. Intell. Human. Comput.* (2021) 1–15.
- [20] A. Hassouneh, A. Mutawa, M. Murugappan, Development of a real-time emotion recognition system using facial expressions and EEG based on machine learning and deep neural network methods, *Inf. Med. Unlocked* 20 (2020) 100372.
- [21] H. Zang, S.Y. Foo, S. Bernadin, A. Meyer-Baese, Facial emotion recognition using asymmetric pyramidal networks with gradient centralization, *IEEE Access* 9 (2021) 64487–64498.
- [22] R.-H. Huan, J. Shu, S.-L. Bao, R.-H. Liang, P. Chen, K.-K. Chi, Video multimodal emotion recognition based on Bi-GRU and attention fusion, *Multimed. Tools Appl.* 80 (6) (2021) 8213–8240.
- [23] K. Zhang, Y. Li, J. Wang, Z. Wang, X. Li, Feature Fusion for Multimodal Emotion Recognition Based on Deep Canonical Correlation Analysis, *IEEE Signal Process Lett.* 28 (2021) 1898–1902.
- [24] H. Wen, S. You, Y. Fu, Cross-modal dynamic convolution for multi-modal emotion recognition, *J. Vis. Commun. Image Represent.* 78 (2021) 103178.
- [25] T. Sharma, M. Diwakar, P. Singh, C. Arya, S. Lamba, P. Kumar, in: *IEEE*, 2021, pp. 1–6.
- [26] N.S. Suhaimi, J. Mountstephens, J. Teo, EEG-based emotion recognition: A state-of-the-art review of current trends and opportunities, *Comput. Intell. Neurosci.* 2020 (2020).
- [27] E.P. Torres, E.A. Torres, M. Hernández-Álvarez, S.G. Yoo, EEG-based BCI emotion recognition: a survey, *Sensors* 20 (18) (2020) 5083.
- [28] A. Topic, M. Russo, Emotion recognition based on EEG feature maps through deep learning network, *Eng. Sci. Technol. Int. J.* 24 (6) (2021) 1442–1454.
- [29] E.H. Houssein, A. Hammad, A.A. Ali, Human emotion recognition from EEG-based brain-computer interface using machine learning: a comprehensive review, *Neural Comput. & Applic.* (2022) 1–31.
- [30] T. Tuncer, S. Dogan, A. Subasi, LEDPatNet19: Automated emotion recognition model based on nonlinear LED pattern feature extraction function using EEG signals, *Cogn. Neurodyn.* (2021) 1–12.
- [31] A. Subasi, T. Tuncer, S. Dogan, D. Tanko, U. Sakoglu, EEG-based emotion recognition using tunable Q wavelet transform and rotation forest ensemble classifier, *Biomed. Signal Process. Control* 68 (2021) 102648.
- [32] A. Dogan, et al., PrimePatNet87: prime pattern and tunable q-factor wavelet transform techniques for automated accurate EEG emotion recognition, *Comput. Biol. Med.* 138 (2021) 104867.
- [33] T. Tuncer, S. Dogan, A. Subasi, A new fractal pattern feature generation function based emotion recognition method using EEG, *Chaos Solitons Fractals* 144 (2021) 110671.
- [34] D. Huang, S. Chen, C. Liu, L. Zheng, Z. Tian, D. Jiang, Differences first in asymmetric brain: A bi-hemisphere discrepancy convolutional neural network for EEG emotion recognition, *Neurocomputing* 448 (2021) 140–151.
- [35] Y. Tan, Z. Sun, F. Duan, J. Solé-Casals, C.F. Caiafa, A multimodal emotion recognition method based on facial expressions and electroencephalography, *Biomed. Signal Process. Control* 70 (2021) 103029.
- [36] H. Zhang, Expression-EEG based collaborative multimodal emotion recognition using deep autoencoder, *IEEE Access* 8 (2020) 164130–164143.
- [37] X. Wu, W.-L. Zheng, Z. Li, B.-L. Lu, Investigating EEG-based functional connectivity patterns for multimodal emotion recognition, *J. Neural Eng.* 19 (1) (2022) 016012.
- [38] "EMOTIV | Brain Data Measuring Hardware and Software Solutions."
- [39] D.L. Guarín, et al., Toward an automatic system for computer-aided assessment in facial palsy, *Facial Plastic Surg. Aesthet. Med.* 22 (1) (2020) 42–49.
- [40] J.J. Kim, S.L. Parker, J.R. Doty, R. Cunningham, P. Gilbert, J.N. Kirby, Neurophysiological and behavioural markers of compassion, *Sci. Rep.* 10 (1) (2020) 1–9.
- [41] R.A. Clark, B.F. Mentiplay, E. Hough, Y.H. Pua, Three-dimensional cameras and skeleton pose tracking for physical function assessment: A review of uses, validity, current developments and Kinect alternatives, *Gait Posture* 68 (2019) 193–200.
- [42] M. Wei, S. Roodenrys, L. Miller, E. Barkus, Complex scenes from the International Affective Picture System (IAPS): Agreement-based emotional categories, *Exp. Psychol.* 67 (3) (2020) 194.
- [43] S. Nakakoga, H. Higashi, J. Muramatsu, S. Nakachi, T. Minami, Asymmetrical characteristics of emotional responses to pictures and sounds: Evidence from pupillometry, *PLoS One* 15 (4) (2020) e0230775.